WWW.ATMIA.PUT.POZNAN.PL AMTM VOL. 36 (2016) 7-11

ARCHIVES OF MECHANICAL TECHNOLOGY AND MATERIALS

Laser alloying of bearing steel with boron and self-lubricating addition

Mateusz Kotkowiak[a], Adam Piasecki[a], Michał Kulka[a*]

[a] *Poznan University of Technology, Piotrowo 3 Street, 60-965 Poznan, Poland*

e-mail address: michal.kulka@put.poznan.pl

A B S T R A C T

100CrMnSi6–4 bearing steel has been widely used for many applications, e.g. rolling bearings which work in difficult operating conditions. Therefore, this steel has to be characterized by special properties such as high wear resistance and high hardness. In this study laser-boriding was applied to improve these properties. Laser alloying was conducted as the two step process with two different types of alloying material: amorphous boron only and amorphous boron with addition of calcium fluoride CaF_2. At first, the surface was coated with paste including alloying material. Second step of the process consisted in laser re-melting. The surface of sample, coated with the paste, was irradiated by the laser beam. In this study, TRUMPF TLF 2600 Turbo CO_2 laser was used. The microstructure, microhardness and wear resistance of both laser-borided layer and laser-borided layer with the addition of calcium fluoride were investigated. The layer, alloyed with boron and CaF_2, was characterized by higher wear resistance than the layer after laser boriding only.

Key words: laser boriding, self-lubricating addition, hardness, wear resistance

1. INTRODUCTION

100CrMnSi6–4 bearing steel is widely used for a lot of practical applications, working under difficult conditions. This steel has a suitable chemical composition which provides very good properties, such as high hardness after hardening, resulting from the high hardenability. Therefore, this steel is often used to produce the rolling bearings.

Nowadays, there is a tendency to improve the tribological properties of this steel, such as friction coefficient and wear resistance. It is very important because otherwise there will be a lot of material losses and it can be very dangerous for the environment and people.

To improve tribological behavior of bearing steel, diamond like carbon coatings (DLC) and deep cryogenic treatment were applied [1, 2]. It was also possible to use PVD and CVD methods [3, 4]. The effects of cooling rate during hardening on the tribological properties were investigated [5].

Self–lubricating additives also provided good tribological properties of surface layers. There were various methods of producing the self-lubricating coatings. Some of them were sintered by SPS. The improved tribological properties of $ZrO_2(Y_2O_3)$ [6] and TiAl [7] matrix composite with addition of solid lubricants were confirmed. Self–lubricating coatings were also produced by plasma spraying [8, 9]. Such composite coatings consisted of graphite/CaF_2/TiC/Ni-based alloy [8] or NiCr/(Cr_3C_2–BaF_2·CaF_2) [9].

Cold pressing and sintering was used to form self-lubricating material [10–12]. The copper–based composites were modified by self– lubricating additives in order to improve their tribological behavior [10]. Aluminum oxide based composites with solid lubricants Al_2O_3–TiC [11] and Al_2O_3/(W, Ti)C/CaF_2 [12] were also cold pressed and sintered.

Hot pressing and sintering was applied to fabrication of Ti–Al self–lubricating material using different amount of solid lubricant [13]. (WAl)C–Co ceramic composite was prepared with lubricant addition using the same method and was investigated under sea water environment [14].

Laser cladding was also successfully used to produce the self-lubricating layers [15, 16, 17]. The composite layer Ni–Cr–C–CaF_2 was deposited on γ–TiAl by this method [15]. Microstructure and tribological properties of laser clad CaF_2/Al_2O_3 wear-resistant ceramic matrix composite coating were investigated [16]. Laser cladding was applied to modify copper by the self-lubricating Co–based alloy/TiC/CaF_2 composite coatings [17].

As it was mentioned above, calcium fluoride was very popular self-lubricating addition. This material belongs to the high temperature lubricants and achieves the best properties above 500°C. Its friction coefficient in room temperature is higher than that-observed in high temperature [18]. CaF_2 is characterized by density 3.18g/cm^3, melting point 1633K [19] and the low shear strength because of crystal structure of this material [20].

In this paper the self-lubricating laser-borided layer, including the addition of calcium fluoride CaF_2, was produced on 100CrMnSi6–4 bearing steel. The microstructure, microhardness and wear resistance were investigated.

2. EXPERIMENTAL PROCEDURE

2.1. Material

The chemical composition of 100CrMnSi6–4 bearing steel was shown in **Table 1**. The specimen was ring-shaped of the dimensions as follows: external diameter – 20 mm, internal diameter – 12 mm and height – 12 mm.

Table 1. Chemical composition of bearing steel 100CrMnSi6–4 [wt %]

C	Cr	Mn	Si	Cu	P	S	Fe
1.03	1.52	1.08	0.59	0.11	0.022	0.012	balance

2.2. Laser alloying

Laser alloying was conducted as the two step process with or without addition of calcium fluoride particles. First step consisted in coating the surface with alloying material, and the second – in laser re-melting. The scheme of laser alloying was presented in Figure 1. At first, the special paste was prepared. Powders, including amorphous boron only or amorphous boron and CaF_2, were blended with polyvinyl alcohol. Then, outer cylindrical surface of the specimen was coated by such a paste. The thickness of the paste was equal to 60 μm, and the amorphous boron and calcium fluoride mass ratio was 10:1.

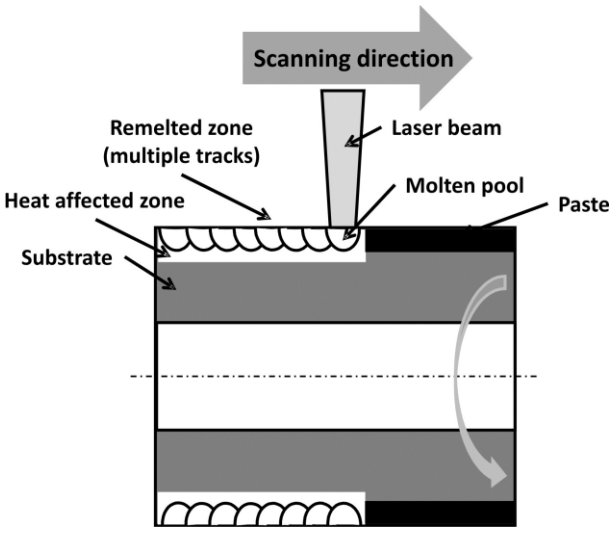

Fig. 1. Scheme of laser alloying

Laser heat treatment (LHT) was carried out as the next step of laser alloying. The laser beam was used for re-melting the cylindrical surface of the specimen coated with paste. This process was performed using the TRUMPF TLF 2600 Turbo CO_2 laser of the nominal power 2.6 kW. The parameters of LHT were as follows: laser beam power (P) 1.17 kW, laser beam diameter (d) 2 mm, and scanning rate (v_l) 2.88 m/min. The scanning rate (v_l) resulted from rotational speed (n) 45.85 min^{-1} and feed rate (v_f) 0.28 mm per revolution. The multiple laser tracks overlapped with distance f = 0.28 mm (**Figure 2**).

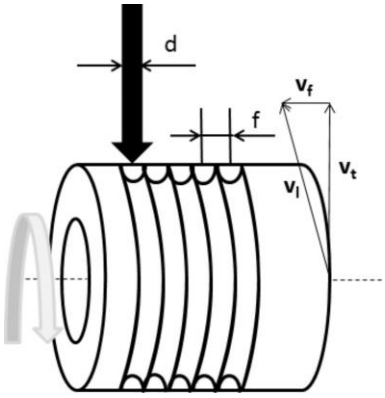

Fig. 2. Scheme of multiple tracks producing: d – laser beam diameter (d=2mm); v_f - rate of feed; v_l – scanning rate; n - rotational speed; v_t – tangential rate; f – distance from track to track

2.3. Microstructure and properties

After the laser alloying the metallographic specimens were prepared. For microstructural observation, the polished and etched cross sections were used. The specimens were polished using abrasive paper with different granularity and, finally, with abrasive slurry, containing Al_2O_3. Next, the specimens were etched by solution which consisted of 5% nital in order to reveal the components of microstructure. The optical microscope (OM) and scanning electron microscope (SEM) techniques were used.

Next the microhardness of the layers was studied by the Vickers method. For these measurements, the apparatus Buehler Micromet II was applied using the load 50 gf (0.49 N). Microhardness profiles were determined perpendicularly to the surface of the specimens.

Wear resistance was studied under condition of dry friction using the MBT-01 device. Frictional pair (**Figure 3**) consisted of the laser-alloyed specimen and plate-shaped counter–specimen made of sintered carbide S20S. Chemical composition of counter-sample was shown in **Table 2**.

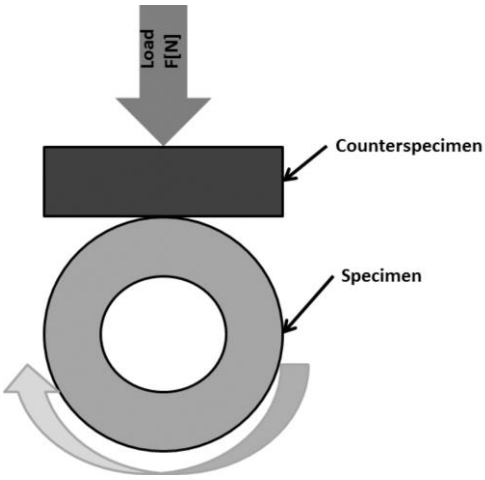

Fig. 3. The scheme of wear resistance test

Table 2. Chemical composition of sintered carbide S20S [wt %]

Material	WC	TiC+TaC+NbC	Co
S20S	58	31.5	10.5

The parameters of wear resistance tests were as follows: load F = 15 kgf (147 N) and speed of the specimen, which was equal to 0.26 m/s, and was resulted from the rotational speed of the sample n = 250min^{-1} and from its external diameter. The wear tests lasted 4 hours. The wear resistance was evaluated by the relative mass loss of the components of frictional pair (sample and counter-sample), according to the equation:

$$\frac{\Delta m}{m_i} = \frac{m_i - m_f}{m_i} \quad (1)$$

where: Δm is mass loss [mg], m_i is initial mass of specimen or counter-specimen [mg], m_f is final mass of specimen or counter-specimen [mg].

Worn surfaces were analyzed with the use of a scanning electron microscope (SEM) equipped with an energy dispersive spectrometer (EDS) PGT Avalon.

3. RESULTS

3.1. Microstructure

The OM images of produced surface layers were shown in **Figure 4**. Regardless of alloying material used, three zones were observed in the microstructure. Close to the surface appeared re-melted zone (MZ), marked as 1. Below MZ, heat-affected zone (HAZ) was visible (2). The last one corresponded to the base material (3).

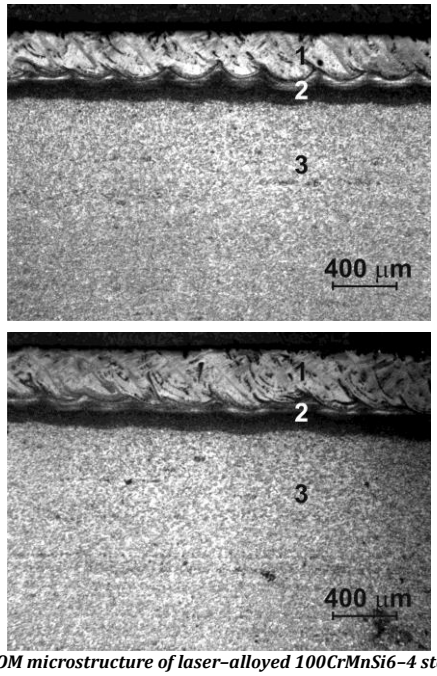

Fig. 4. OM microstructure of laser–alloyed 100CrMnSi6–4 steel: a) with boron, b) with boron and addition of CaF_2

The re-melted zone consisted mainly of eutectic mixture of iron borides and martensite [21, 22]. Besides, the particles of calcium fluoride were observed in MZ in case of addition of this lubricant to alloying material (**Figure 5**). CaF_2 particles were partially re-melted and vaporized, partially re-melted and re-solidified, and some of them weren't subjected to these transformations and stayed in the unchanged cuboidal shape. The thicknesses of MZ were similar: 314 μm for the layer produced after laser boriding only, and 310 μm for the laser-alloyed layer with boron and solid lubricant. Relatively high overlapping (86%) during laser heat treatment was the reason for obtaining the compact surface layers which were free of cracks and gas pores as well as uniform in respect of the thickness. Directly below MZ in HAZ, martensite appeared. Microstructure of HAZ changed within the distance from the surface due to diminishing cooling rate. Therefore, at the end of HAZ, bainite was observed.

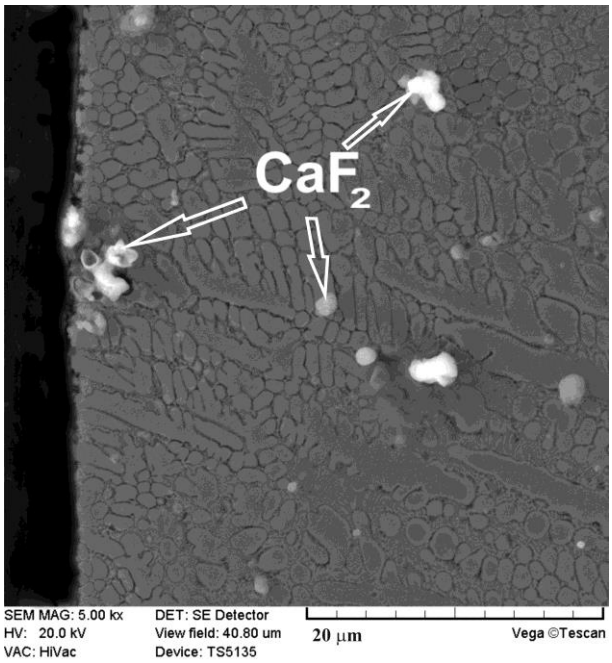

Fig. 5. SE image of re-melted zone in laser–alloyed steel with boron and CaF_2

3.2. Microhardness

The microhardness profiles of laser-borided layer and laser-borided layer with self-lubricant addition were shown in **Figure 6**. Presence of eutectic mixture (martensite and iron borides) in re-melted zone (MZ) caused an increase in surface hardness. Laser-alloyed layer with boron only was characterized by compact boride zone close to the surface (up to depth of 40 μm). As a consequence, the hardness in this zone exceeded 1400 HV0.05. The whole hardness profile for this sample was characterized by slightly higher hardness compared to the profile obtained after laser alloying with boron and calcium fluoride. Hardness of MZ ranged from 1072 to 1413 HV0.05 for laser-alloyed layer with boron and varied between 946 and 1096 HV0.05 for laser-alloyed layer

with boron and CaF_2. The high hardness was also measured directly below MZ due to appearance of martensite in this area of HAZ. The evolution in microstructure of this zone, especially diminished percentage of martensite due to lower cooling rate, caused decrease in hardness within the distance from the surface. However, in case of addition of calcium fluoride to alloying material, the gradient of hardness in this zone was diminished. Such a situation could result in a better bond of the surface layer with the base material as well as in more advantageous stress distribution between laser-alloyed layer and substrate. In base material, the hardness for both layers was equal to approximately 200 HV0.05.

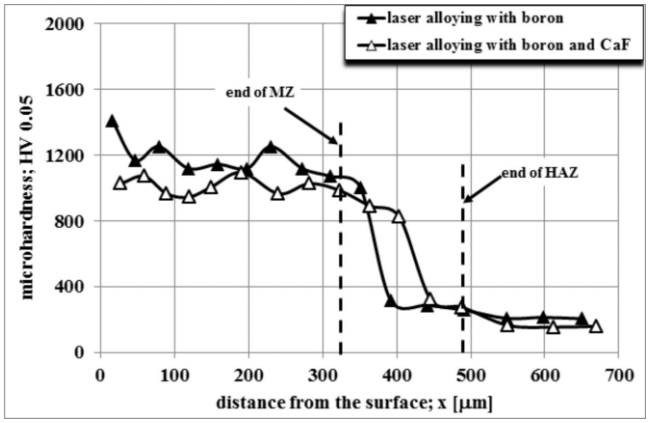

Fig. 6. Microhardness profiles of laser-alloyed layers

3.3. Wear resistance

The results of four-hour wear resistance test were shown in **Table 3**. Wear resistance was evaluated by relative mass loss of specimens and counter-specimens. The smaller value of $\Delta m/m_i$ was measured, the better wear resistance was characteristic of investigated material. The results of measurements were presented in **Table 3**. $\Delta m/m_i$ values of counter-specimens, mating with both surface layers didn't differ significantly. In case of the sample after laser-boriding with addition of self-lubricating particles (CaF_2), the relative loss of mass was about 20% smaller. During the test, on the worn surface of this sample, tribofilm was produced (**Figure 7**).

Table 3. Relative loss of mass of the specimen and counter-specimen

aterial	Relative loss of mass $\Delta m/m_i$	
	Specimen	Counter–specimen
Laser-borided 100CrMnSi6–4 steel with boron	$17.93 \cdot 10^{-4}$	$5.56 \cdot 10^{-4}$
Laser–borided 100CrMnSi6–4 steel with boron and CaF_2	$14.58 \cdot 10^{-4}$	$5.68 \cdot 10^{-4}$

EDS pattern of calcium indicated the areas of increased concentration of this element. Particles of CaF_2 were smeared on the worn surface. It was the reason for diminished wear and, as a consequence, wear resistance improved. However, tribofilm didn't cover the whole worn surface. Therefore, in the regions, in which tribofilm was relatively thin or invisible, the intensive abrasive wear proceeded, assuming the shape of shallow grooves.

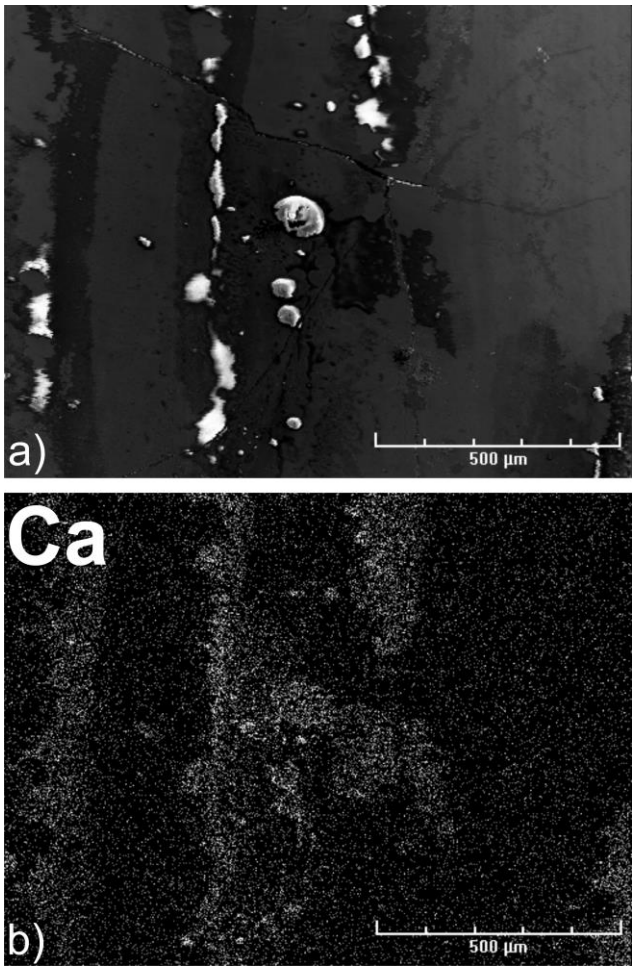

Fig. 7. Worn surface of sample after laser-boriding with addition of calcium fluoride: a) SE image of worn surface, b) EDS pattern of Ca

4. CONCLUSIONS

Self-lubricating layer was produced on the 100CrMnSi6–4 bearing steel using the laser alloying with boron and CaF_2. Two layers were produced: first with boron only and second with boron and with addition of calcium fluoride CaF_2. Microstructure of this layer as well as some properties, such as microhardness and wear resistance, were compared to those-obtained for typical laser-borided layer without calcium fluoride. Microstructure of the laser-alloyed steel consisted of three zones: re-melted zone (MZ), heat-affected zone (HAZ) and base material. Re-melted zone contained mainly eutectic mixture of martensite and iron borides. In case of laser alloying with boron and calcium fluoride, the particles of CaF_2 were additionally observed in this zone. Microstructure of HAZ changed within the distance from the

surface. Directly below MZ, martensite appeared whereas bainite was visible at the end of HAZ. High overlapping (86%) during laser modification was the reason for obtaining the surface layers which were uniform in respect of the thickness. The thicknesses of the re-melted zone were similar, irrespective of addition of solid lubricant. The microhardness of laser-alloyed layers was different. The addition of soft CaF_2 phase caused the decrease in microhardness of MZ in comparison with the layer alloyed with boron only. However, the diminished hardness gradient was characteristic of HAZ in this case. Addition of CaF_2 particles had an advantageous influence on wear resistance. The relative loss of mass was lower for sample after boriding with solid-lubricant addition. On the worn surface the tribofilm appeared which provided lubrication between friction pair. The presence of tribofilm was proved by the EDS method. In areas, in which tribofilm didn't occur, the intensive abrasive wear proceeded.

REFERENCES

[1] Podgornik B., Vižintin J., Borovšak U., Megušar F., Tribological properties of DLC coatings in helium, Tribol. Lett. 47(2) (2012) 223-230.

[2] Gunes I., Cicek A., Aslantas K., Effect of Deep Cryogenic Treatment on Wear Resistance of AISI 52100 Bearing Steel, Trans. Indian Inst. Met. 67(6) (2014) 909–917.

[3] Podgornik B., Borovsak U, Megusar F., Kosir K., Performance of low-friction coatings in helium environments, Surface & Coatings Technology 206 (2012) 4651-4658.

[4] Nilsson M., Olsson M., Tribological testing of some potential PVD and CVD coatings for steel wire drawing dies, Wear 273 (2011) 55–59.

[5] Polat S., Türedi E., Atapek Ş.H., Köseoğlu M., Wear behavior of heat treated DIN 100Cr6 steels, International Iron and Steel Symposium Karabük, Türkiye, 02-04 April 2012, 181-196.

[6] Ouyang J.H., Li Y.F., Wang Y.M., Zhou Y., Murakami T., Sasaki S., Microstructure and tribological properties of ZrO2(Y2O3) matrix composites doped with different solid lubricants from room temperature to 800ºC, Wear 267 (2009) 1353–1360.

[7] Shi X., Yao J., Xu Z., Zhai W., Song S., Wang M., Zhang Q., Tribological performance of TiAl matrix self-lubricating composites containing Ag, Ti3SiC2 and BaF2/CaF2 tested from room temperature to 600ºC, Materials and Design 53 (2014) 620–633.

[8] Cai B., Tan Y.-F., He L., Tan H.,. Wang X.-L., Tribological behavior and mechanisms of graphite/CaF2/TiC/Ni-base alloy composite coatings, Trans. Nonferrous Met. Soc. China 23 (2013) 392–399.

[9] Huang C., Lu D., Zhang W., Friction and Wear Characteristics of Plasma-Sprayed Self-Lubrication Coating with Clad Powder at Elevated Temperatures up to 800ºC, Journal of Thermal Spray Technology 23(3) (2014) 463-469.

[10] Konopka K., Roik T.A., Gavrish A.P., Vitsuk Yu.Yu., Mazan T., Effect of CaF2 surface layers on the friction behavior of copper-based composite, Powder Metallurgy and Metal Ceramics 51(5-6) (2012) 363-367.

[11] Yang X., Wang Z., Song P., Cheng J., Gu J., Ma T., Dry Sliding Wear Behavior of Al2O3-TiC Ceramic Composites Added with Solid Lubricant CaF2 by Cold Pressing and Sintering, Tribology Transactions 58 (2015) 231-239.

[12] Xu C.H., Wu G.Y., Xiao G.C., Fang B., Al2O3/(W,Ti)C/CaF2 multi-component graded self-lubricating ceramic cutting tool material, Int. Journal of Refractory Metals and Hard Materials 45 (2014) 125–129.

[13] Wang X., Yang L., Wang S., Zhang Y., Tribological properties of Ti-Al. Alloy self-lubricating composite materials, Advanced Materials Research Vol. 842 (2014) pp 114-117.

[14] Kong L., Cheng J., Jin K., Yin B., Qiao Z., Yang J., Friction and wear properties of (WAl)C–Co ceramic composites under sea water environment, Ceramics International

[15] Liu W.-G.,. Liu X.-B, Zhang Z.-G., Guo J., Development and characterization of composite Ni–Cr–C–CaF2 laser cladding on TiAl intermetallic alloy, Journal of Alloys and Compounds 470 (2009) L25–L28.

[16] Wang H.M., Yu Y.L., Li S.Q., Microstructure and tribological properties of laser clad CaF2/Al2O3 self-lubrication wear-resistant ceramic matrix composite coatings, Scripta Materialia 47 (2002) 57–61.

[17] Yan H., Zhang J., Zhang P., Yu Z., Li C., Xu P., Lu Y., Laser cladding of Co-based alloy/TiC/CaF2 self-lubricating composite coatings on copper for continuous casting mold, Surface & Coatings Technology 232 (2013) 362–369.

[18] Yang J.-F., Jiang Y., Hardell J., Prakash B., Fang Q.-F., Influence of service temperature on tribological characteristics of self-lubricant coatings: A review. Front. Mater. Sci. 7(1) (2013) 28-39.

[19] Kobayashi T., Maruyama T., Yasuda T., Sliding Properties of Composite Sprayed Coating between Bronze Powder and Solid Lubricant, Materials Transactions 44(5) (2003) 1024-1028.

[20] Jianxin D., Tongkun C., Xuefeng Y., Jianhua L., Junlong S., Jinlong Z., Wear behavior and self tribofilm formation of hot-pressed Al2O3/TiC/CaF2 ceramic composites sliding against cemented carbide, Ceramics International 33 (2007) 213–220.

[21] Kulka M., Makuch N., Pertek A., Microstructure and properties of laser-borided 41Cr4 steel, Optics and Laser Technology 45 (2013) 308-318

[22] Kulka M., Makuch N., Dziarski P., Mikołajczak D., Przestacki. D., Gradient boride layers formed by diffusion carburizing and laser boriding, Optics and Lasers in Engineering 67 (2015) 163-175